

Study of scalar meson $f_0(980)$ and $K_0^*(1430)$ from $B \rightarrow f_0(980)\rho(\omega, \phi)$ and $B \rightarrow K_0^*(1430)\rho(\omega)$ decays

Zhi-Qing Zhang*

Department of Physics, Henan University of Technology, Zhengzhou, Henan 450052, People's Republic of China
(Received 29 June 2010; published 31 August 2010)

In the two-quark model supposition for $f_0(980)$ and $K_0^*(1430)$, the branching ratios and the direct CP -violating asymmetries for decays $\bar{B}^0 \rightarrow f_0(980)\rho^0(\omega, \phi)$, $K_0^{*0}(1430)\rho^0(\omega)$, $K_0^{*-}(1430)\rho^+$ and $B^- \rightarrow f_0(980)\rho^-$, $K_0^{*0}(1430)\rho^-$, $K_0^{*-}(1430)\rho^0(\omega)$ are studied by employing the perturbative QCD factorization approach. We find the following results: (a) if the scalar meson $f_0(980)$ is viewed as a mixture of $s\bar{s}$ and $(u\bar{u} + d\bar{d})/\sqrt{2}$, the branching ratios of the $b \rightarrow d$ transition processes $\bar{B}^0 \rightarrow f_0(980)\rho^0(\omega, \phi)$ and $B^- \rightarrow f_0(980)\rho^-$ are smaller than the currently experimental upper limits, and the predictions for the decays $\bar{B}^0 \rightarrow f_0(980)\omega$, $B^- \rightarrow f_0(980)\rho^-$ are not far away from their limits; (b) in the $b \rightarrow s$ transition processes $B \rightarrow K_0^*(1430)\rho(\omega)$, the branching ratio of $\bar{B}^0 \rightarrow K_0^{*0}(1430)\rho^0$ is the smallest one, at the order of 10^{-7} by treating $K_0^*(1430)$ as the lowest lying state, about 4.8×10^{-6} by considering $K_0^*(1430)$ as the first excited state; (c) the direct CP -violating asymmetries of decays $B \rightarrow f_0(980)\rho(\omega)$ have a strong dependence on the mixing angle θ : they are large in the range of $25^\circ < \theta < 40^\circ$, and small in the range of $140^\circ < \theta < 165^\circ$, while the direct CP -violating asymmetry amplitudes of decays $B \rightarrow K_0^*(1430)\rho(\omega)$ are not large in the two kinds of state supposition for $K_0^*(1430)$ and most of them are less than 20%.

DOI: 10.1103/PhysRevD.82.034036

PACS numbers: 13.25.Hw, 12.38.Bx, 14.40.Nd

I. INTRODUCTION

Along with many scalar mesons that are found in experiments, more and more efforts have been made to study the scalar meson spectrum theoretically [1–7]. Today, it is still a difficult but interesting topic. Our most important task is to uncover the mysterious structure of the scalar mesons. There are two typical schemes for the classification of them [1,2]. Scenario I (SI): the nonet mesons below 1 GeV, including $f_0(600)$, $f_0(980)$, $K^*(800)$, and $a_0(980)$, are usually viewed as the lowest lying $q\bar{q}$ states, while the nonet ones near 1.5 GeV, including $f_0(1370)$, $f_0(1500)/f_0(1700)$, $K^*(1430)$, and $a_0(1450)$, are suggested as the first excited states. In scenario II (SII), the nonet mesons near 1.5 GeV are treated as $q\bar{q}$ ground states, while the nonet mesons below 1 GeV are exotic states beyond the quark model such as four-quark bound states.

The production of the scalar mesons from B meson decays provides a different unique insight to the inner structures of these mesons. It provides various factorization approaches a new usefulness. The QCD factorization (QCDF) approach [8,9] has been used to systematically study the B meson decays with a scalar meson involved in the final states. The authors draw the conclusion that scenario II is more preferable than scenario I; that is to say, the light scalar mesons below 1 GeV are possible four-quark bound states and the scalar mesons near 1.5 GeV are the lowest lying $q\bar{q}$ states. If $f_0(980)$ is a four-quark bound state, it requires the pick up of two energetic quark-antiquark pairs to form this scalar meson, so one expects

that the $B \rightarrow f_0(980)X$ rate might be smaller in the four-quark model than in the two-quark picture. From the previous calculations [8,10], we also expect that the two-quark component of $f_0(980)$ plays an essential role for $B \rightarrow f_0(980)\rho(\omega, \phi)$ decays. Just like the QCDF approach, in order to make a quantitative prediction, we assume the scalar meson $f_0(980)$ as a mixture of $s\bar{s}$ and $n\bar{n}(\equiv (u\bar{u} + d\bar{d})/\sqrt{2})$; that is

$$|f_0(980)\rangle = |s\bar{s}\rangle \cos\theta + |n\bar{n}\rangle \sin\theta, \quad (1)$$

where θ is the $f_0 - \sigma$ mixing angle. In the phenomenological and experimental analyses [11,12], θ lies in the ranges of $25^\circ < \theta < 40^\circ$ and $140^\circ < \theta < 165^\circ$. Certainly, $K_0^*(1430)$ can be treated as a $q\bar{q}$ state in both SI and SII, so we will calculate $B \rightarrow K_0^*(1430)\rho(\omega)$ decays in two scenarios.

On the experimental side, for $f_0(980)$ emerging as a pole of the amplitude in the S wave [13], many channels such as $B \rightarrow f_0(980)K$ can be obtained by the fitting of Dalitz plots of the decays $B \rightarrow \pi^+ \pi^- K$ and $B \rightarrow \bar{K} K K$ and so on [14–17]. Although many decay channels that involved $f_0(980)$ in the final states have been measured over the years, it has yet not been possible to account for its inner structure. For the decays $B \rightarrow f_0(980)\rho(\omega, \phi)$, only the upper limits are available now [18,19]:

$$\begin{aligned} \text{Br}(B^- \rightarrow f_0(980)\rho^-) &< 3.8 \times 10^{-6}, \\ \text{Br}(\bar{B}^0 \rightarrow f_0(980)\rho^0) &< 1.06 \times 10^{-6}, \\ \text{Br}(\bar{B}^0 \rightarrow f_0(980)\omega) &< 3.0 \times 10^{-6}, \\ \text{Br}(\bar{B}^0 \rightarrow f_0(980)\phi) &< 7.6 \times 10^{-7}. \end{aligned} \quad (2)$$

*zhangzhiqing@haut.edu.cn

It is noticed that we have assumed $\text{Br}(f_0(980) \rightarrow \pi^+ \pi^-) = 0.50$ to obtain the upper data. For the decays $B \rightarrow K_0^*(1430)\rho(\omega)$, there is still no experimental result.

Here we would like to use the perturbative QCD (PQCD) approach to study $f_0(980)$ and $K_0^*(1430)$ in the decays $B \rightarrow f_0(980)\rho(\omega, \phi)$ and $B \rightarrow K_0^*(1430)\rho(\omega)$. In the following, $f_0(980)$ and $K_0^*(1430)$ are denoted as f_0 and K_0^* in some places for convenience. The layout of this paper is as follows. In Sec. II, the relevant decay constants and light-cone distribution amplitudes of relevant mesons are introduced. In Sec. III, we then analyze these decay channels using the PQCD approach. The numerical results and the discussions are given in Sec. IV. The conclusions are presented in the final part.

II. DECAY CONSTANTS AND DISTRIBUTION AMPLITUDES

For the wave function of the heavy B meson, we take

$$\Phi_B(x, b) = \frac{1}{\sqrt{2N_c}} (\not{P}_B + m_B) \gamma_5 \phi_B(x, b). \quad (3)$$

Here only the contribution of the Lorentz structure $\phi_B(x, b)$ is taken into account, since the contribution of the second Lorentz structure $\bar{\phi}_B$ is numerically small [20] and has been neglected. For the distribution amplitude $\phi_B(x, b)$ in Eq. (3), we adopt the model

$$\phi_B(x, b) = N_B x^2 (1-x)^2 \exp\left[-\frac{M_B^2 x^2}{2\omega_b^2} - \frac{1}{2}(\omega_b b)^2\right], \quad (4)$$

where ω_b is a free parameter, and the value of the normalization factor is taken as $N_B = 91.745$ for $\omega_b = 0.4$ in numerical calculations.

In the two-quark picture, the vector decay constant f_S and the scalar decay constant \bar{f}_S for a scalar meson S can be defined as

$$\langle S(p) | \bar{q}_2 \gamma_\mu q_1 | 0 \rangle = f_S p_\mu, \quad (5)$$

$$\langle S(p) | \bar{q}_2 q_1 | 0 \rangle = m_S \bar{f}_S, \quad (6)$$

where $m_S(p)$ is the mass (momentum) of the scalar meson. The relation between f_S and \bar{f}_S is

$$\frac{m_S}{m_2(\mu) - m_1(\mu)} f_S = \bar{f}_S, \quad (7)$$

where $m_{1,2}$ are the running current quark masses. For the neutral scalar meson f_0 , owing to charge conjugation invariance or the G parity conservation, it cannot be produced via the vector current, so $f_{f_0} = 0$. Taking the mixing into account, Eq. (6) is changed to

$$\begin{aligned} \langle f_0^n | \bar{d}d | 0 \rangle &= \langle f_0^n | \bar{u}u | 0 \rangle = \frac{1}{\sqrt{2}} m_{f_0} \tilde{f}_{f_0}^n, \\ \langle f_0^n | \bar{s}s | 0 \rangle &= m_{f_0} \tilde{f}_{f_0}^s. \end{aligned} \quad (8)$$

Because the decay constants $\tilde{f}_{f_0}^n$ and $\tilde{f}_{f_0}^s$ are very close [8], we assume that $\tilde{f}_{f_0}^n = \tilde{f}_{f_0}^s$ and denote them as \bar{f}_{f_0} in the following. For the scalar meson $K_0^*(1430)$, $f_{K_0^*}$ will get a very small value after the $SU(3)$ symmetry breaking being considered. The light-cone distribution amplitudes for the scalar meson S can be written as

$$\begin{aligned} \langle S(p) | \bar{q}_1(z) q_2(0) | 0 \rangle &= \frac{1}{\sqrt{2N_c}} \int_0^1 dx e^{ixp \cdot z} \{ \not{p} \Phi_S(x) + m_S \Phi_S^S(x) \\ &\quad + m_S (\not{n}_+ \not{n}_- - 1) \Phi_S^T(x) \}_{j\bar{l}}, \end{aligned} \quad (9)$$

here n_+ and n_- are lightlike vectors: $n_+ = (1, 0, 0_T)$, $n_- = (0, 1, 0_T)$, and n_+ is parallel with the moving direction of the scalar meson. The normalization can be related to the decay constants:

$$\begin{aligned} \int_0^1 dx \Phi_S(x) &= \int_0^1 dx \Phi_S^T(x) = 0, \\ \int_0^1 dx \Phi_S^S(x) &= \frac{\bar{f}_S}{2\sqrt{2N_c}}. \end{aligned} \quad (10)$$

The twist-2 light-cone distribution amplitude Φ_S can be expanded in the Gegenbauer polynomials:

$$\begin{aligned} \Phi_S(x, \mu) &= \frac{\bar{f}_S(\mu)}{2\sqrt{2N_c}} 6x(1-x) \\ &\quad \times \left[B_0(\mu) + \sum_{m=1}^{\infty} B_m(\mu) C_m^{3/2}(2x-1) \right], \end{aligned} \quad (11)$$

where the decay constants and the Gegenbauer moments B_1, B_3 of distribution amplitudes for $f_0(980)$ and $K_0^*(1430)$ have been calculated in the QCD sum rules [8]. These values are all scale dependent and specified below:

$$\text{scenario I: } B_1(K_0^*) = 0.58 \pm 0.07, \quad B_3(K_0^*) = -1.2 \pm 0.08, \quad \bar{f}_{K_0^*} = -(300 \pm 30) \text{ MeV}, \quad (12)$$

$$B_1(f_0) = -0.78 \pm 0.08, \quad B_3(f_0) = 0.02 \pm 0.07, \quad \bar{f}_{f_0} = -(370 \pm 20) \text{ MeV}; \quad (13)$$

$$\text{scenario II: } B_1(K_0^*) = -0.57 \pm 0.13, \quad B_3(K_0^*) = 0.42 \pm 0.22, \quad \bar{f}_{K_0^*} = -(445 \pm 50) \text{ MeV}, \quad (14)$$

which are taken by fixing the scale at 1 GeV.

As for the twist-3 distribution amplitudes Φ_S^S and Φ_S^T , we adopt the asymptotic form:

$$\Phi_S^S = \frac{1}{2\sqrt{2N_c}} \bar{f}_S, \quad \Phi_S^T = \frac{1}{2\sqrt{2N_c}} \bar{f}_S(1-2x). \quad (15)$$

The distribution amplitudes up to twist-3 of the vector mesons are

$$\begin{aligned} & \langle V(P, \epsilon_L^*) | \bar{q}_{2\beta}(z) q_{1\alpha}(0) | 0 \rangle \\ &= \frac{1}{2N_C} \int_0^1 dx e^{ixP \cdot z} [M_V \epsilon_L^\mu \Phi_V(x) + \epsilon_L^\mu \not{P} \Phi_V^t(x) \\ &+ M_V \Phi_V^s(x)]_{\alpha\beta}, \end{aligned} \quad (16)$$

for longitudinal polarization. The distribution amplitudes can be parametrized as

$$\Phi_V(x) = \frac{2f_V}{\sqrt{2N_C}} [1 + a_2^{\parallel} C_2^{3/2}(2x-1)], \quad (17)$$

$$\Phi_V^t(x) = \frac{3f_V^T}{2\sqrt{2N_C}} (2x-1)^2, \quad (18)$$

$$\phi_V^s(x) = -\frac{3f_V^T}{2\sqrt{2N_C}} (2x-1),$$

where the decay constant f_V [21] and the transverse decay constant f_V^T [22] are given as the following values:

$$\begin{aligned} f_\rho &= 209 \pm 2 \text{ MeV}, & f_\omega &= 195 \pm 3 \text{ MeV}, \\ f_\phi &= 231 \pm 4 \text{ MeV}, \end{aligned} \quad (19)$$

$$\begin{aligned} f_\rho^T &= 165 \pm 9 \text{ MeV}, & f_\omega^T &= 151 \pm 9 \text{ MeV}, \\ f_\phi^T &= 186 \pm 9 \text{ MeV}. \end{aligned} \quad (20)$$

Here the Gegenbauer polynomial is defined as $C_2^{3/2}(t) = \frac{3}{2}(5t^2 - 1)$. For the Gegenbauer moments, we quote the numerical results as [23]

$$a_{2\rho}^{\parallel} = a_{2\omega}^{\parallel} = 0.15 \pm 0.07, \quad a_{2\phi}^{\parallel} = 0.18 \pm 0.08. \quad (21)$$

III. THE PERTURBATIVE QCD CALCULATION

Under the two-quark model for the scalar mesons f_0 and K_0^* supposition, the decay amplitude for $B \rightarrow VS$, where V represents ρ , ω , ϕ and S represents f_0 , K_0^* , can be conceptually written as the convolution

$$\begin{aligned} \mathcal{A}(B \rightarrow VS) &\sim \int d^4k_1 d^4k_2 d^4k_3 \text{Tr}[C(t)\Phi_B(k_1)\Phi_V(k_2) \\ &\times \Phi_S(k_3)H(k_1, k_2, k_3, t)], \end{aligned} \quad (22)$$

where k_i 's are momenta of the antiquarks included in each

mesons, and Tr denotes the trace over Dirac and color indices. $C(t)$ is the Wilson coefficient which results from the radiative corrections at short distance. In the above convolution, $C(t)$ includes the harder dynamics at a larger scale than the M_B scale and describes the evolution of local 4-Fermi operators from m_W (the W boson mass) down to the $t \sim \mathcal{O}(\sqrt{\bar{\Lambda}M_B})$ scale, where $\bar{\Lambda} \equiv M_B - m_b$. The function $H(k_1, k_2, k_3, t)$ describes the four-quark operator and the spectator quark connected by a hard gluon whose q^2 is in the order of $\bar{\Lambda}M_B$, and includes the $\mathcal{O}(\sqrt{\bar{\Lambda}M_B})$ hard dynamics. Therefore, this hard part H can be perturbatively calculated. The functions $\Phi_{(V,S)}$ are the wave functions of the vector meson V and the scalar meson S , respectively.

Since the b quark is rather heavy, we consider the B meson at rest for simplicity. It is convenient to use light-cone coordinate (p^+, p^-, \mathbf{p}_T) to describe the meson's momenta,

$$p^\pm = \frac{1}{\sqrt{2}}(p^0 \pm p^3), \quad \text{and} \quad \mathbf{p}_T = (p^1, p^2). \quad (23)$$

Using these coordinates, the B meson and the two final state meson momenta can be written as

$$P_B = \frac{M_B}{\sqrt{2}}(1, 1, \mathbf{0}_T), \quad P_2 = \frac{M_B}{\sqrt{2}}(1 - r_S^2, r_V^2, \mathbf{0}_T), \quad (24)$$

$$P_3 = \frac{M_B}{\sqrt{2}}(r_S^2, 1 - r_V^2, \mathbf{0}_T),$$

respectively, where the ratio $r_{S(V)} = m_{S(V)}/M_B$, and $m_{S(V)}$ is the scalar meson S (the vector meson V) mass. Putting the antiquark momenta in B , V , and S mesons as k_1 , k_2 , and k_3 , respectively, we can choose

$$\begin{aligned} k_1 &= (x_1 P_1^+, 0, \mathbf{k}_{1T}), & k_2 &= (x_2 P_2^+, 0, \mathbf{k}_{2T}), \\ k_3 &= (0, x_3 P_3^-, \mathbf{k}_{3T}). \end{aligned} \quad (25)$$

For these considered decay channels, the integration over k_1^- , k_2^- , and k_3^+ in Eq. (22) will lead to

$$\begin{aligned} \mathcal{A}(B \rightarrow VS) &\sim \int dx_1 dx_2 dx_3 b_1 db_1 b_2 db_2 b_3 db_3 \\ &\cdot \text{Tr}[C(t)\Phi_B(x_1, b_1)\Phi_V(x_2, b_2) \\ &\times \Phi_S(x_3, b_3)H(x_i, b_i, t)S_i(x_i)e^{-S(t)}], \end{aligned} \quad (26)$$

where b_i is the conjugate space coordinate of k_{iT} , and t is the largest energy scale in function $H(x_i, b_i, t)$. In order to smear the end-point singularity on x_i , the jet function $S_i(x)$ [24], which comes from the resummation of the double logarithms $\ln^2 x_i$, is used. The last term $e^{-S(t)}$ in Eq. (26) is the Sudakov form factor which suppresses the soft dynamics effectively [25].

For the considered decays, the related weak effective Hamiltonian H_{eff} can be written as [26]

$$\mathcal{H}_{\text{eff}} = \frac{G_F}{\sqrt{2}} \left[\sum_{p=u,c} V_{pb} V_{pq}^* (C_1(\mu) O_1^p(\mu) + C_2(\mu) O_2^p(\mu)) - V_{tb} V_{tq}^* \sum_{i=3}^{10} C_i(\mu) O_i(\mu) \right], \quad (27)$$

where $q = d, s$. Here the Fermi constant $G_F = 1.16639 \times 10^{-5} \text{ GeV}^{-2}$, and the functions $Q_i (i = 1, \dots, 10)$ are the local four-quark operators. We specify below the operators in \mathcal{H}_{eff} for the $b \rightarrow q$ transition:

$$\begin{aligned} O_1^\mu &= \bar{q}_\alpha \gamma^\mu L u_\beta \cdot \bar{u}_\beta \gamma_\mu L b_\alpha, \\ O_2^\mu &= \bar{q}_\alpha \gamma^\mu L u_\alpha \cdot \bar{u}_\beta \gamma_\mu L b_\beta, \\ O_3 &= \bar{q}_\alpha \gamma^\mu L b_\alpha \cdot \sum_{q'} \bar{q}'_\beta \gamma_\mu L q'_\beta, \\ O_4 &= \bar{q}_\alpha \gamma^\mu L b_\beta \cdot \sum_{q'} \bar{q}'_\beta \gamma_\mu L q'_\alpha, \\ O_5 &= \bar{q}_\alpha \gamma^\mu L b_\alpha \cdot \sum_{q'} \bar{q}'_\beta \gamma_\mu R q'_\beta, \\ O_6 &= \bar{q}_\alpha \gamma^\mu L b_\beta \cdot \sum_{q'} \bar{q}'_\beta \gamma_\mu R q'_\alpha, \\ O_7 &= \frac{3}{2} \bar{q}_\alpha \gamma^\mu L b_\alpha \cdot \sum_{q'} e_{q'} \bar{q}'_\beta \gamma_\mu R q'_\beta, \\ O_8 &= \frac{3}{2} \bar{q}_\alpha \gamma^\mu L b_\beta \cdot \sum_{q'} e_{q'} \bar{q}'_\beta \gamma_\mu R q'_\alpha, \\ O_9 &= \frac{3}{2} \bar{q}_\alpha \gamma^\mu L b_\alpha \cdot \sum_{q'} e_{q'} \bar{q}'_\beta \gamma_\mu L q'_\beta, \\ O_{10} &= \frac{3}{2} \bar{q}_\alpha \gamma^\mu L b_\beta \cdot \sum_{q'} e_{q'} \bar{q}'_\beta \gamma_\mu L q'_\alpha, \end{aligned} \quad (28)$$

where α and β are the $SU(3)$ color indices; L and R are the left- and right-handed projection operators with $L = (1 - \gamma_5)$, $R = (1 + \gamma_5)$. The sum over q' runs over the quark fields that are active at the scale $\mu = O(m_b)$, i.e., ($q' \in \{u, d, s, c, b\}$).

In Fig. 1, we give the leading order Feynman diagrams for the channel $\bar{B}^0 \rightarrow \rho^0 f_0(980)$ as an example. The Feynman diagrams for the other decays are similar and not given in order to make a brief version. For the same purpose, the detailed analytic formulas for the diagrams of each decays are not presented and can be obtained from those of $B \rightarrow f_0(980) K^*$ [27] by replacing corresponding wave functions and parameters.

Combining the contributions from different diagrams, the total decay amplitudes for these decays can be written as

$$\begin{aligned} \mathcal{M}(\bar{B} \rightarrow f_0 \rho(\phi, \omega)) &= \mathcal{M}_{s\bar{s}}(f_0 \rho(\phi, \omega)) \\ &\quad \times \cos\theta + \frac{1}{\sqrt{2}} \mathcal{M}_{n\bar{n}}(f_0 \rho(\phi, \omega)) \\ &\quad \times \sin\theta, \end{aligned} \quad (29)$$

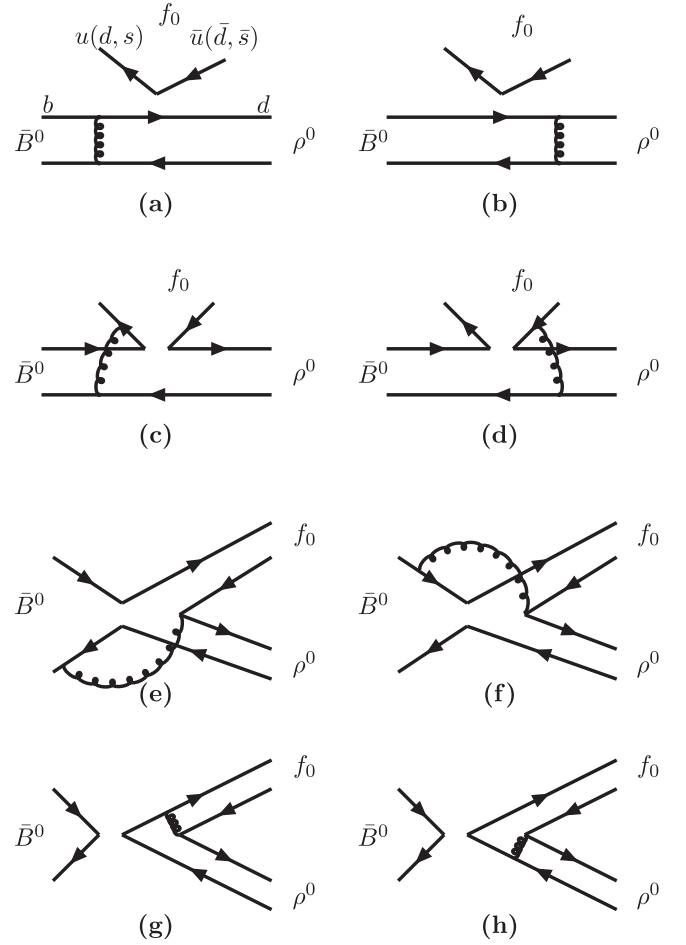


FIG. 1. Diagrams contributing to the decay $\bar{B}^0 \rightarrow \rho^0 f_0(980)$.

where θ is mixing angle and

$$\begin{aligned} \sqrt{2} \mathcal{M}_{s\bar{s}}(f_0 \rho^0) &= -\mathcal{M}_{n\bar{n}}(f_0 \rho^-) \\ &= \xi_t M_{e\rho} \left(C_4 - \frac{1}{2} C_{10} \right) \\ &\quad + \xi_t M_{e\rho}^{P2} \left(C_6 - \frac{1}{2} C_8 \right), \end{aligned} \quad (30)$$

$$\begin{aligned} \sqrt{2} \mathcal{M}_{s\bar{s}}(f_0 \omega) &= -\xi_t M_{e\rho} \left(C_4 - \frac{1}{2} C_{10} \right) \\ &\quad - \xi_t M_{e\rho}^{P2} \left(C_6 - \frac{1}{2} C_8 \right), \end{aligned} \quad (31)$$

$$\begin{aligned} \mathcal{M}_{s\bar{s}}(f_0 \phi) &= -\xi_t \left[(M_{a\phi} + M_{af_0}) \left(C_4 - \frac{1}{2} C_{10} \right) \right. \\ &\quad + (M_{a\phi}^{P2} + M_{af_0}^{a f_0}) \left(C_6 - \frac{1}{2} C_8 \right) \\ &\quad \left. + (F_{af_0} + F_{a\phi}) \left(a_3 - a_5 + \frac{1}{2} a_7 - \frac{a_9}{2} \right) \right], \end{aligned} \quad (32)$$

$$\begin{aligned}
\sqrt{2}\mathcal{M}_{n\bar{n}}(f_0\rho^0) = & \left\{ \xi_u[(M_{ef_0} + M_{af_0} - M_{e\rho} + M_{a\rho})C_2 + (F_{ef_0} + F_{af_0} + F_{a\rho})a_2] \right. \\
& - \xi_t \left[F_{ef_0} \left(-a_4 + \frac{3}{2}C_7 + \frac{1}{2}C_8 + \frac{5}{3}C_9 + C_{10} \right) + (F_{a\rho} + F_{af_0}) \left(-a_4 - \frac{3}{2}C_7 - \frac{1}{2}C_8 + \frac{5}{3}C_9 + C_{10} \right) \right. \\
& - (F_{a\rho}^2 + F_{af_0}^2 + F_{e\rho}^2) \left(a_6 - \frac{1}{2}a_8 \right) + (M_{ef_0} + M_{af_0} + M_{a\rho}) \left(\frac{1}{2}C_9 + \frac{3}{2}C_{10} - C_3 \right) \\
& - M_{e\rho} \left(C_3 + 2C_4 - \frac{1}{2}C_9 + \frac{1}{2}C_{10} \right) - (M_{ef_0}^{P1} + M_{e\rho}^{P1} + M_{af_0}^{P1} + M_{a\rho}^{P1}) \left(C_5 - \frac{1}{2}C_7 \right) - M_{e\rho}^{P2} \left(2C_6 + \frac{1}{2}C_8 \right) \\
& \left. \left. + (M_{ef_0}^{P2} + M_{af_0}^{P2} + M_{a\rho}^{P2}) \frac{3}{2}C_8 \right] \right\}, \tag{33}
\end{aligned}$$

$$\begin{aligned}
\mathcal{M}_{n\bar{n}}(f_0\rho^-) = & \left\{ \xi_u[M_{ef_0}C_2 + (M_{af_0} + M_{e\rho} + M_{a\rho})C_1 + F_{ef_0}a_2 + (F_{af_0} + F_{a\rho})a_1] \right. \\
& - \xi_t \left[F_{e\rho}^2 \left(a_6 - \frac{1}{2}a_8 \right) + (F_{a\rho} + F_{ef_0} + F_{af_0})(a_4 + a_{10}) + (F_{a\rho}^2 + F_{af_0}^2)(a_6 + a_8) \right. \\
& + (M_{ef_0} + M_{af_0} + M_{a\rho})(C_3 + C_9) + M_{e\rho} \left(C_3 + 2C_4 - \frac{1}{2}C_9 + \frac{1}{2}C_{10} \right) \\
& \left. \left. + (M_{ef_0}^{P1} + M_{af_0}^{P1} + M_{a\rho}^{P1})(C_5 + C_7) + M_{e\rho}^{P1} \left(C_5 - \frac{1}{2}C_7 \right) + M_{e\rho}^{P2} \left(2C_6 + \frac{1}{2}C_8 \right) \right] \right\}, \tag{34}
\end{aligned}$$

$$\begin{aligned}
\sqrt{2}\mathcal{M}_{n\bar{n}}(f_0\omega) = & \left\{ \xi_u[(M_{ef_0} + M_{af_0} + M_{e\rho} + M_{a\rho})C_2 + (F_{ef_0} + F_{af_0} + F_{a\rho})a_2] \right. \\
& - \xi_t \left[(F_{ef_0} + F_{a\rho} + F_{af_0}) \left(\frac{7}{3}C_3 + \frac{5}{3}C_4 - 2C_5 - \frac{2}{3}C_6 - \frac{1}{2}C_7 - \frac{1}{6}C_8 + \frac{1}{3}C_9 - \frac{1}{3}C_{10} \right) \right. \\
& + (F_{a\rho}^2 + F_{af_0}^2 + F_{e\rho}^2) \left(a_6 - \frac{1}{2}a_8 \right) + (M_{e\rho} + M_{ef_0} + M_{af_0} + M_{a\rho}) \left(C_3 + 2C_4 - \frac{1}{2}C_9 + \frac{1}{2}C_{10} \right) \\
& \left. \left. + (M_{ef_0}^{P1} + M_{e\rho}^{P1} + M_{af_0}^{P1} + M_{a\rho}^{P1}) \left(C_5 - \frac{1}{2}C_7 \right) + (M_{ef_0}^{P2} + M_{af_0}^{P2} + M_{a\rho}^{P2} + M_{e\rho}^{P2}) \left(2C_6 + \frac{1}{2}C_8 \right) \right] \right\}, \tag{35}
\end{aligned}$$

$$\mathcal{M}_{n\bar{n}}(f_0\phi) = -\xi_t \left[F_{ef_0} \left(a_3 + a_5 - \frac{a_7}{2} - \frac{a_9}{2} \right) + M_{ef_0} \left(C_4 - \frac{C_{10}}{2} \right) + M_{ef_0}^{P2} \left(C_6 - \frac{C_8}{2} \right) \right]; \tag{36}$$

$$\begin{aligned}
\sqrt{2}\mathcal{M}(K^{*-}\rho^0) = & \xi_u[(M_{e\rho} + M_{a\rho})C_1 + M_{eK^*}C_2 + F_{a\rho}a_1 + F_{eK^*}a_2] \\
& - \xi_t \left[F_{e\rho}^2(a_6 + a_8) + F_{eK^*} \left(\frac{3}{2}(C_7 + C_9) + \frac{1}{2}(C_8 + C_{10}) \right) + (M_{e\rho} + M_{a\rho})(C_3 + C_9) \right. \\
& \left. + (M_{e\rho}^{P1} + M_{a\rho}^{P1})(C_5 + C_7) + F_{a\rho}(a_4 + a_{10}) + F_{a\rho}^2(a_6 + a_8) + M_{eK^*} \frac{3}{2}C_{10} + M_{eK^*}^{P2} \frac{3}{2}C_8 \right], \tag{37}
\end{aligned}$$

$$\begin{aligned}
\sqrt{2}\mathcal{M}(K^{*-}\omega) = & \xi_u[(M_{e\omega} + M_{a\omega})C_1 + M_{eK^*}C_2 + F_{a\omega}a_1 + F_{eK^*}a_2] \\
& - \xi_t \left[F_{e\omega}^2(a_6 + a_8) + F_{eK^*} \left(2(C_3 + C_5) + \frac{2}{3}(C_4 + C_6) + \frac{1}{2}(C_9 + C_7) + \frac{1}{6}(C_8 + C_{10}) \right) \right. \\
& + (M_{e\omega} + M_{a\omega})(C_3 + C_9) + (M_{e\omega}^{P1} + M_{a\omega}^{P1})(C_5 + C_7) + F_{a\omega}(a_4 + a_{10}) + F_{a\omega}^2(a_6 + a_8) \\
& \left. + M_{eK^*} \left(2C_4 + \frac{1}{2}C_{10} \right) + M_{eK^*}^{P2} \left(2C_6 + \frac{1}{2}C_8 \right) \right], \tag{38}
\end{aligned}$$

$$\begin{aligned} \mathcal{M}(K^{*0}\rho^-) = & \xi_u[M_{a\rho}C_1 + F_{a\rho}a_1] - \xi_t\left[F_{e\rho}^{P2}(a_6 + a_8) + M_{e\rho}\left(C_3 - \frac{C_9}{2}\right) + M_{a\rho}(\Psi C_3 + C_9) + M_{e\rho}^{P1}\left(C_5 - \frac{C_7}{2}\right)\right. \\ & \left. + M_{a\rho}^{P1}(C_5 + C_7) + F_{a\rho}(a_4 + a_{10}) + F_{a\rho}^{P2}(a_6 + a_8)\right], \end{aligned} \quad (39)$$

$$\begin{aligned} \sqrt{2}\mathcal{M}(K^{*0}\rho^0) = & \xi_u[M_{eK^*}C_2 + F_{eK^*}a_2] - \xi_t\left[F_{e\rho}^{P2}\left(a_6 - \frac{1}{2}a_8\right) + F_{eK^*}\left(\frac{3}{2}(C_7 + C_9) + \frac{1}{2}(C_8 + C_{10})\right)\right. \\ & + (M_{e\rho} + M_{a\rho})\left(C_3 - \frac{1}{2}C_9\right) + (M_{e\rho}^{P1} + M_{a\rho}^{P1})\left(C_5 - \frac{1}{2}C_7\right) + F_{a\rho}\left(a_4 - \frac{1}{2}a_{10}\right) + F_{a\rho}^{P2}\left(a_6 - \frac{1}{2}a_8\right) \\ & \left. + M_{eK^*}\frac{3}{2}C_{10} + M_{eK^*}^{P2}\frac{3}{2}C_8\right], \end{aligned} \quad (40)$$

$$\begin{aligned} \sqrt{2}\mathcal{M}(K^{*0}\omega) = & \xi_u[M_{eK^*}C_2 + F_{eK^*}a_2] - \xi_t\left[F_{e\omega}^{P2}\left(a_6 - \frac{1}{2}a_8\right) + (M_{e\omega} + M_{a\omega})\left(C_3 - \frac{1}{2}C_9\right)\right. \\ & + F_{eK^*}\left(2(C_3 + C_5) + \frac{2}{3}(C_4 + C_6) + \frac{1}{2}(C_9 + C_7) + \frac{1}{6}(C_8 + C_{10})\right) + (M_{e\omega}^{P1} + M_{a\omega}^{P1})\left(C_5 - \frac{1}{2}C_7\right) \\ & \left. + F_{a\omega}\left(a_4 - \frac{1}{2}a_{10}\right) + F_{a\omega}^{P2}\left(a_6 - \frac{1}{2}a_8\right) + M_{eK^*}\left(2C_4 + \frac{1}{2}C_{10}\right) + M_{eK^*}^{P2}\left(2C_6 + \frac{3}{2}C_8\right)\right], \end{aligned} \quad (41)$$

$$\begin{aligned} \mathcal{M}(K^{*-}\rho^+) = & \xi_u M_{e\rho}C_1 - \xi_t\left[F_{e\rho}^{P2}(a_6 + a_8) + M_{e\rho}(C_3 + C_9) + M_{a\rho}\left(C_3 - \frac{C_9}{2}\right) + M_{e\rho}^{P1}(C_5 + C_7) + M_{a\rho}^{P1}\left(C_5 - \frac{C_7}{2}\right)\right. \\ & \left. + F_{a\rho}\left(a_4 - \frac{a_{10}}{2}\right) + F_{a\rho}^{P2}\left(a_6 - \frac{a_8}{2}\right)\right]. \end{aligned} \quad (42)$$

The combinations of the Wilson coefficients are defined as usual [28]:

$$\begin{aligned} a_1(\mu) &= C_2(\mu) + \frac{C_1(\mu)}{3}, \\ a_2(\mu) &= C_1(\mu) + \frac{C_2(\mu)}{3}, \\ a_i(\mu) &= C_i(\mu) + \frac{C_{i+1}(\mu)}{3}, \quad i = 3, 5, 7, 9, \\ a_i(\mu) &= C_i(\mu) + \frac{C_{i-1}(\mu)}{3}, \quad i = 4, 6, 8, 10. \end{aligned} \quad (43)$$

IV. NUMERICAL RESULTS AND DISCUSSIONS

We use the following input parameters in the numerical calculations [18,29]:

$$\begin{aligned} f_B = 190 \text{ MeV}, \quad M_B = 5.28 \text{ GeV}, \\ M_W = 80.41 \text{ GeV}, \end{aligned} \quad (44)$$

$$V_{ub} = |V_{ub}|e^{-i\gamma} = 3.93 \times 10^{-3}e^{-i68^\circ}, \quad V_{tb} = 1.0, \quad (45)$$

$$\begin{aligned} V_{td} = |V_{td}|e^{-i\beta} = 8.1 \times 10^{-3}e^{-i21.6^\circ}, \\ V_{us} = 0.2255, \end{aligned} \quad (46)$$

$$V_{ts} = 0.0387, \quad V_{ud} = 0.974, \quad (47)$$

$$\tau_{B^\pm} = 1.671 \times 10^{-12} \text{ s},$$

$$\tau_{B^0} = 1.530 \times 10^{-12} \text{ s}. \quad (48)$$

In the B -rest frame, the decay rates of $B \rightarrow f_0(980)\rho(\omega, \phi)$, $K_0^*(1430)\rho(\omega)$ can be written as

$$\Gamma = \frac{G_F^2}{32\pi m_B} |\mathcal{M}|^2 (1 - r_S^2), \quad (49)$$

where \mathcal{M} is the total decay amplitude of each considered decay and r_S the mass ratio, which have been given in Sec. III.

If $f_0(980)$ is purely composed of $n\bar{n}(s\bar{s})$, the branching ratios of $B^- \rightarrow f_0(980)\rho^-$ and $\bar{B}^0 \rightarrow f_0(980)\rho^0(\omega, \phi)$ are

$$\mathcal{B}(B^- \rightarrow f_0(980)(n\bar{n})\rho^-) = (7.5_{-0.8}^{+0.9+1.4+1.4}) \times 10^{-6}, \quad (50)$$

$$\mathcal{B}(\bar{B}^0 \rightarrow f_0(980)(n\bar{n})\rho^0) = (1.1_{-0.1-0.2-0.3}^{+0.2+0.3+0.2}) \times 10^{-6}, \quad (51)$$

$$\mathcal{B}(\bar{B}^0 \rightarrow f_0(980)(n\bar{n})\omega) = (5.3_{-0.5-0.9-0.6}^{+0.5+1.1+0.9}) \times 10^{-6}, \quad (52)$$

$$\mathcal{B}(\bar{B}^0 \rightarrow f_0(980)(n\bar{n})\phi) = (1.7_{-0.2-0.4-0.3}^{+0.2+0.5+0.3}) \times 10^{-9}, \quad (53)$$

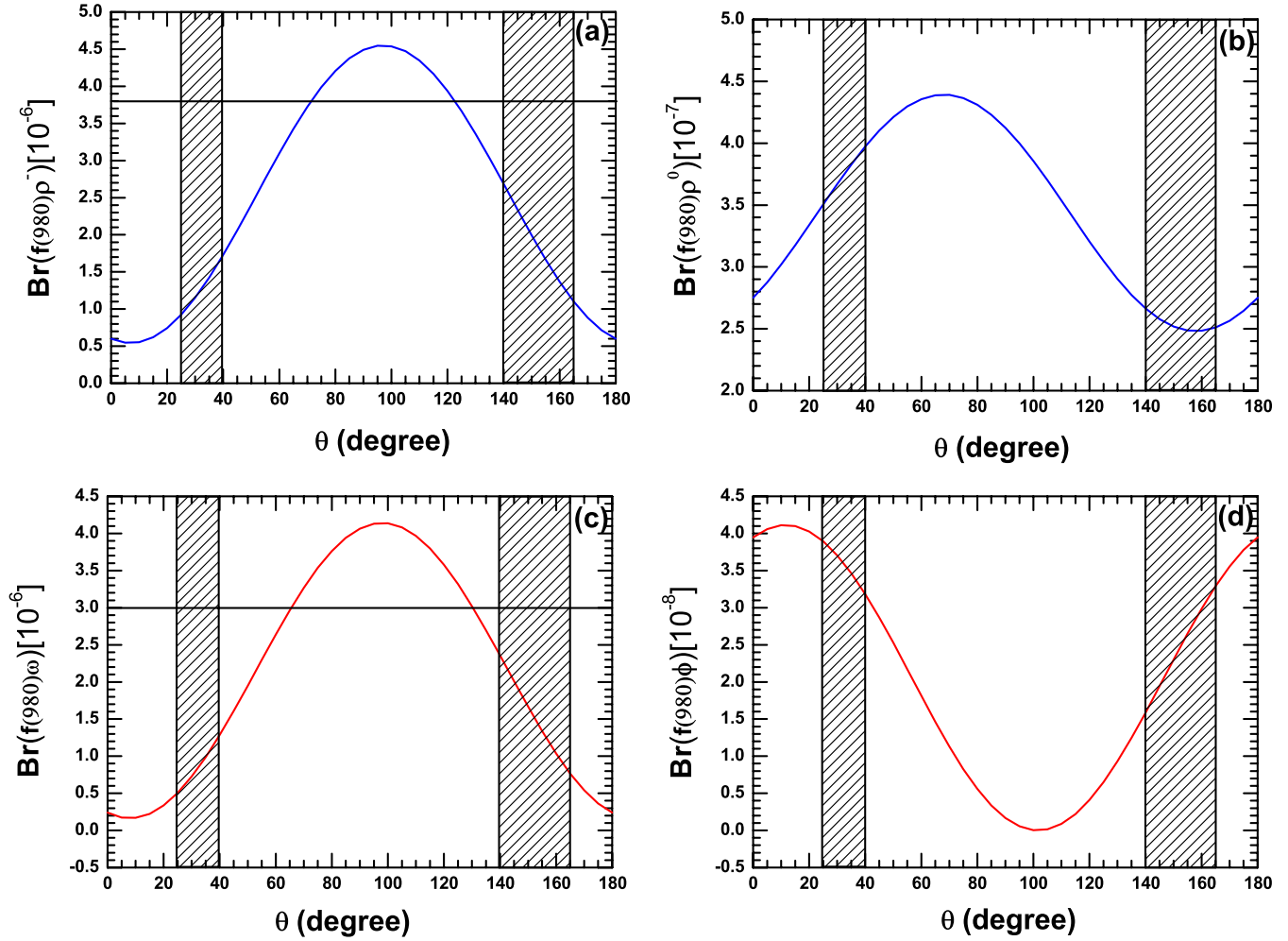


FIG. 2 (color online). The dependence of the branching ratios for $B_s^- \rightarrow f_0(980)\rho^-$ (a), $\bar{B}^0 \rightarrow f_0(980)\rho^0$ (b), $\bar{B}^0 \rightarrow f_0(980)\omega$ (c), and $\bar{B}^0 \rightarrow f_0(980)\phi$ (d) on the mixing angle θ using the inputs derived from QCD sum rules. The horizontal solid lines show the experimental upper limits. The vertical bands show two possible ranges of θ : $25^\circ < \theta < 40^\circ$ and $140^\circ < \theta < 165^\circ$.

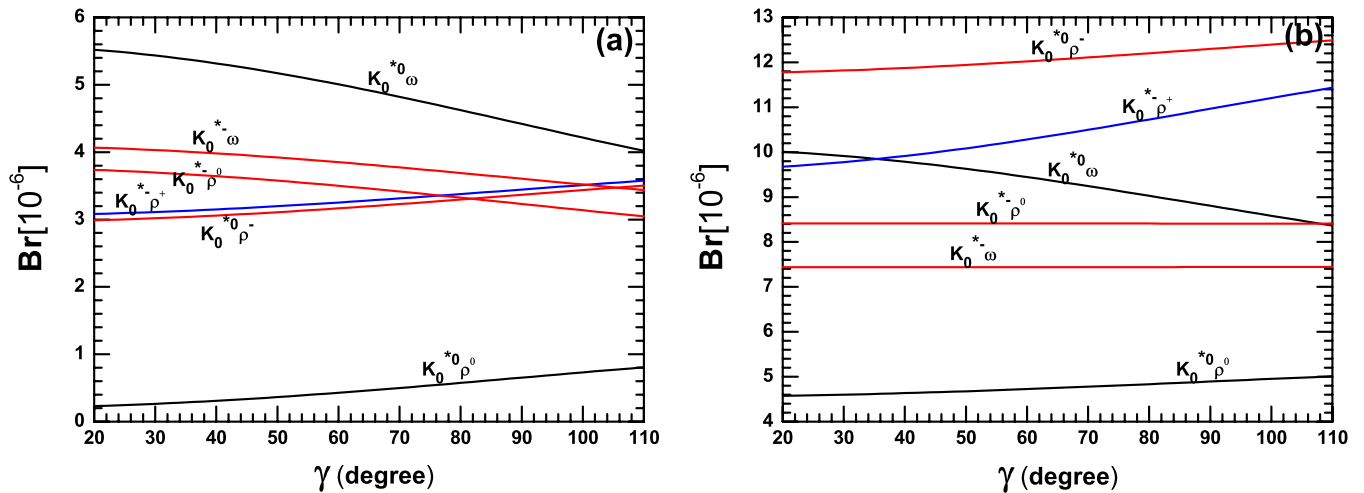


FIG. 3 (color online). The dependence of the branching ratios for $B^- \rightarrow K_0^{*0}\rho^-, K_0^{*-}\rho^0, K_0^{*-}\omega$ and $\bar{B}^0 \rightarrow K_0^{*-}\rho^+, K_0^{*0}\rho^0, K_0^{*0}\omega$ on the Cabibbo-Kobayashi-Maskawa angle γ .

$$\mathcal{B}(B^- \rightarrow f_0(980)(s\bar{s})\rho^-) = (3.0_{-0.3-0.6-0.4}^{+0.3+0.7+0.5}) \times 10^{-7}, \quad (54)$$

$$\mathcal{B}(\bar{B}^0 \rightarrow f_0(980)(s\bar{s})\rho^0) = (1.4_{-0.2-0.3-0.2}^{+0.3+0.3+0.2}) \times 10^{-7}, \quad (55)$$

$$\mathcal{B}(\bar{B}^0 \rightarrow f_0(980)(s\bar{s})\omega) = (1.2_{-0.1-0.2-0.2}^{+0.1+0.3+0.2}) \times 10^{-7}, \quad (56)$$

$$\mathcal{B}(\bar{B}^0 \rightarrow f_0(980)(s\bar{s})\phi) = (2.0_{-0.2-0.3-0.1}^{+0.2+0.4+0.0}) \times 10^{-8}, \quad (57)$$

where the uncertainties are from the decay constant of $f_0(980)$, the Gegenbauer moments B_1, B_3 , and the B meson shape parameter $\omega = 0.40 \pm 0.04$ GeV. In these $b \rightarrow d$ transition processes, the decay $\bar{B}^0 \rightarrow f_0(980)\phi$ is very different from the other three channels: the value of $\mathcal{B}(B \rightarrow f_0(n\bar{n})\phi)$ is smaller than that of $\mathcal{B}(\bar{B} \rightarrow f_0(s\bar{s})\phi)$ by about one order, it is contrary to the cases of the other three decays, at the same time, the branching ratios for $n\bar{n}$ and $s\bar{s}$ components of this channel are both very small.

In Fig. 2, we plot the branching ratios of the considered decays as functions of the mixing angle θ . One can find our predictions for the decays $B^- \rightarrow f_0(980)\rho^-$ and $\bar{B}^0 \rightarrow f_0(980)\omega$ are smaller than the experimental upper limits, but not far away from them. In these decay channels, the branch ratio of $B^- \rightarrow f_0(980)\rho^-$ is the largest one, most possible in the range $(1.0 \sim 2.5) \times 10^{-6}$. We predict that the branch ratio of the decay $\bar{B}^0 \rightarrow f_0(980)\rho^0$ is at the order of 10^{-7} . The tree operator contributions of different diagrams are destructive inference, which leads the tree dominated decay $\bar{B}^0 \rightarrow f_0(980)\rho^0$ to receive a rather small rate. On the contrary, the different amplitudes of the decay $\bar{B}^0 \rightarrow f_0(980)\omega$ are constructive inference and this channel has a larger rate, which is close to the branch ratio of

$B^- \rightarrow f_0(980)\rho^-$. Certainly, this scheme (the inference between different tree contributions) is influenced by the value of the mixing angle; for example, it is not obvious for $\theta = 20^\circ$, while it is obvious for $25^\circ < \theta < 40^\circ$ and $140^\circ < \theta < 165^\circ$. As to the decay $\bar{B}^0 \rightarrow f_0(980)\phi$, there are no tree contributions in the leading order and the contributions from the $s\bar{s}$ component are documented. One can see that its branching ratio is very small and has a different dependence on the mixing angle with other three decays. Its theoretical value is in the range

$$2.2 \times 10^{-8} < \mathcal{B}(\bar{B}^0 \rightarrow f_0(980)\rho) < 3.8 \times 10^{-8}, \quad (58)$$

for $25^\circ < \theta < 40^\circ$;

$$4.6 \times 10^{-8} < \mathcal{B}(\bar{B}^0 \rightarrow f_0(980)\rho) < 6.0 \times 10^{-8}, \quad (59)$$

for $140^\circ < \theta < 165^\circ$,

which is far smaller than its upper limit 38×10^{-8} .

For comparison, we also give the theoretical results in the QCDF framework [9], which are listed in Table I. Obviously, there exists stark disagreement with the QCDF predictions. It mainly arises from taking different values about the decay constants of the scalar mesons and dealing with the annihilation diagram contributions in different way.

As to the decays $B^- \rightarrow K_0^{*0}\rho^-, K_0^{*-}\rho^0, K_0^{*-}\omega$ and $\bar{B}^0 \rightarrow K_0^{*0}\rho^+, K_0^{*0}\rho^0, K_0^{*0}\omega$, we plot their branching ratios as functions of the Cabibbo-Kobayshi-Maskawa angle γ (shown in Fig. 3). Though there are no the experimental results, our argument is that the branch ratios of decays $B \rightarrow K_0^*(1430)\rho(\omega)$ might not be far away from those of $B \rightarrow K\rho(\omega)$, just like the relationship between $B \rightarrow K_0^*(1430)\phi$ and $B \rightarrow K\phi$ [30]. It is not like the channels $B \rightarrow f_0(980)\rho(\omega)$, where there exists large destructive

TABLE I. Branching ratios (in units of 10^{-6}) of $B \rightarrow f_0(980)\rho(\omega, \phi)$ and $B \rightarrow K_0^*(1430)\rho(\omega)$. The theoretical errors correspond to the uncertainties due to (i) the scalar meson decay constants, (ii) the Gegenbauer moments B_1 and B_3 for the scalar mesons, (iii) the B meson shape parameter ω . In order to compare with the QCDF predictions, we also give the predicted branching ratios of $B \rightarrow f_0(980)\rho(\omega, \phi)$ for the $f_0 - \sigma$ mixing angle $\theta = 20^\circ$. For the QCDF results, the branching ratios of $B \rightarrow f_0(980)V$ are in SI, ones of $B \rightarrow K_0^*(1430)V$ are in SII.

Mode	QCDF	Scenario I	Scenario II	Exp.
$B^- \rightarrow f_0(980)\rho^-$	$1.3_{-0.1-0.3-0.1}^{+0.1+0.4+0.1}$	$0.7_{-0.0-0.1-0.1}^{+0.1+0.2+0.2}$		< 3.8
$\bar{B}^0 \rightarrow f_0(980)\rho^0$	$0.01_{-0.00-0.00-0.01}^{+0.00+0.00+0.02}$	$0.33_{-0.03-0.05-0.06}^{+0.04+0.07+0.06}$		< 1.06
$\bar{B}^0 \rightarrow f_0(980)\phi$...	$0.04_{-0.004-0.007-0.003}^{+0.005+0.008+0.000}$		< 0.76
$\bar{B}^0 \rightarrow f_0(980)\omega$	$0.06_{-0.01-0.00-0.02}^{+0.02+0.00+0.02}$	$0.34_{-0.04-0.06-0.05}^{+0.03+0.06+0.06}$		< 3.0
$B^- \rightarrow \bar{K}_0^{*0}(1430)\rho^-$	$66.2_{-19.5-2.4-26.3}^{+25.0+2.8+70.8}$	$3.2_{-0.6-0.7-0.2}^{+0.7+0.8+0.4}$	$12.1_{-0.0-3.1-0.5}^{+2.8+3.9+0.5}$	
$B^- \rightarrow K_0^{*-}(1430)\rho^0$	$21.0_{-5.9-1.1-10.1}^{+7.3+1.2+29.4}$	$3.4_{-0.6-0.5-0.4}^{+0.8+0.7+0.6}$	$8.4_{-0.0-3.2-0.7}^{+2.3+3.3+0.9}$	
$B^- \rightarrow K_0^{*-}(1430)\omega$	$16.1_{-4.0-0.6-8.3}^{+4.9+0.7+22.5}$	$3.8_{-0.9-0.6-0.7}^{+0.9+0.5+0.8}$	$7.4_{-1.5-2.3-0.4}^{+2.1+3.0+0.9}$	
$\bar{B}^0 \rightarrow \bar{K}_0^{*0}(1430)\rho^0$	$36.8_{-11.0-0.7-9.1}^{+14.3+0.9+23.4}$	$0.47_{-0.12-0.17-0.02}^{+0.12+0.20+0.03}$	$4.8_{-0.0-1.0-0.3}^{+1.1+1.0+0.3}$	
$\bar{B}^0 \rightarrow K_0^{*-}(1430)\rho^+$	$51.0_{-13.1-1.2-23.8}^{+16.1+1.4+68.6}$	$3.3_{-0.6-0.8-0.2}^{+0.7+0.8+0.2}$	$10.5_{-0.0-2.6-0.3}^{+2.7+3.5+0.3}$	
$\bar{B}^0 \rightarrow K_0^{*0}(1430)\omega$	$15.6_{-3.7-0.8-5.3}^{+4.4+1.0+14.6}$	$4.9_{-1.1-0.7-0.9}^{+1.2+0.7+1.1}$	$9.3_{-2.0-2.9-1.0}^{+2.1+3.6+1.2}$	

TABLE II. Decay amplitudes for decays $B^- \rightarrow K_0^{*-}(1430)\omega$, $\bar{B}^0 \rightarrow K_0^{*0}(1430)\omega$ ($\times 10^{-2} \text{ GeV}^3$).

	$F_{e\omega}$	$M_{e\omega}^T$	$M_{e\omega}$	$M_{a\omega}^T$	$M_{a\omega}$	$F_{a\omega}^T$
$B^- \rightarrow K_0^{*-}(1430)\omega$ (SI)	0.6	13.2 - 18.4i	-0.5 + 0.7i	12.3 - 12.0i	-0.3 + 0.5i	-1.7 - 2.2i
$\bar{B}^0 \rightarrow K_0^{*0}(1430)\omega$ (SI)	0.6	...	-0.8 + 1.2i	...	-0.7 + 0.8i	...
$B^- \rightarrow K_0^{*-}(1430)\omega$ (SII)	-0.9	-17.3 - 14.6i	0.6 + 0.5i	-13.8 - 0.8i	0.5 - 0.1i	-0.2 + 0.3i
$\bar{B}^0 \rightarrow K_0^{*0}(1430)\omega$ (SII)	-0.9	...	1.1 + 0.9i	...	0.9 - 0.1i	...
	$F_{a\omega}$	$F_{eK^*}^T$	F_{eK^*}	$M_{eK^*}^T$	M_{eK^*}	$F^T + M^T$
$B^- \rightarrow K_0^{*-}(1430)\omega$ (SI)	-3.5 - 2.2i	-32.4	-2.3	-11.0 + 6.3i	-0.6 + 0.3i	-18.5 - 25.6i
$\bar{B}^0 \rightarrow K_0^{*0}(1430)\omega$ (SI)	-3.5 - 2.0i	-32.4	-2.3	-11.0 + 6.3i	-0.6 + 0.3i	-43.4 + 6.3i
$B^- \rightarrow K_0^{*-}(1430)\omega$ (SII)	2.9 + 5.9i	41.2	3.1	0.1 + 6.1i	0.0 + 0.4i	10.0 - 9.0i
$\bar{B}^0 \rightarrow K_0^{*0}(1430)\omega$ (SII)	3.1 + 6.2i	41.2	3.1	0.1 + 6.1i	0.0 + 0.4i	41.3 + 6.1i

(constructive) interference between the components $u\bar{u}$ and $d\bar{d}$ in the mesons $f_0(980)$ and ρ^0 (ω). There exists relatively small interference in decays $B \rightarrow K_0^*(1430)\rho(\omega)$, so the branching ratios of these decays are close to each other; most of them are in the range of $(3 \sim 5) \times 10^{-6}$ for scenario I, and in the range of $(7 \sim 10) \times 10^{-6}$ for scenario II. The branch ratio of $\bar{B}^0 \rightarrow K_0^{*0}(1430)\rho^0$ is the smallest one in these decays, and its value is at the order of 10^{-7} in scenario I. Certainly, we only calculate the leading order diagrams and do not consider the higher order corrections. If the future experimental value about this channel is larger than our prediction, say 10^{-6} , it indicates that this decay might be more sensitive to next-to-leading order corrections, and it is similar to the decays $B^0 \rightarrow \pi^0\pi^0$, $\rho^0\rho^0$. On the contrary, the decay $\bar{B}^0 \rightarrow K_0^{*0}(1430)\omega$ arrives at a large rate in our leading order calculations, especially in scenario I. We expect that its value will be smaller after considering next-to-leading order corrections. In Table II, we list the values of the factorizable and nonfactorizable amplitudes from the emission and annihilation topology diagrams of the decays $B^- \rightarrow K_0^{*-}(1430)\omega$ and $\bar{B}^0 \rightarrow K_0^{*0}(1430)\omega$. $F_{e(a)\omega}$ and $M_{e(a)\omega}$ are the $K_0^*(1430)$ emission (annihilation) factorizable contributions and nonfactorizable contributions from penguin operators, respectively. Similarly, $F_{e(a)K_0^*}$ and $M_{e(a)K_0^*}$ denote the contributions from ω emission (annihilation) factorizable contributions and nonfactorizable contributions from penguin operators, respectively. The upper label “T” denotes the contributions from tree operators. For the ω emission-type diagrams, these two decays have the same Wilson coefficients, so the corresponding amplitudes have the same values. The column “ $F^T + M^T$ ” is for the total tree contribution of factorizable and nonfactorizable diagrams. From Table II, one can find that the tree contributions from ω and K^* emission-type diagrams are destructive in the charged decay, and a smaller real part of the total tree contribution survives in comparison with the neutral one, which makes the branching ratio of $\bar{B}^0 \rightarrow K_0^{*0}(1430)\omega$ larger than that of $B^- \rightarrow K_0^{*-}(1430)\omega$.

Now, we turn to the evaluations of the direct CP -violating asymmetries of the considered decays in

the PQCD approach. The direct CP -violating asymmetry can be defined as

$$\mathcal{A}_{CP}^{\text{dir}} = \frac{|\bar{\mathcal{M}}|^2 - |\mathcal{M}|^2}{|\mathcal{M}|^2 + |\bar{\mathcal{M}}|^2}. \quad (60)$$

From Fig. 4, one can see the direct CP -violating asymmetry values for the decays $B^- \rightarrow f_0(980)\rho^-$ and $\bar{B}^0 \rightarrow f_0(980)\rho^0$ in these two possible ranges of the mixing angle θ are very different, that is to say, their CP -violating asymmetries are sensitive to the mixing angle. For the decay $\bar{B}^0 \rightarrow f_0(980)\omega$, its CP -violating asymmetry is not so sensitive to the mixing angle. If the mixing angle is in the range $25^\circ < \theta < 40^\circ$, the direct CP -violating asymmetries of these decays are about

$$80\% < \mathcal{A}_{CP}^{\text{dir}}(B^- \rightarrow f_0(980)\rho^-) < 90\%, \quad (61)$$

$$-60\% < \mathcal{A}_{CP}^{\text{dir}}(\bar{B}^0 \rightarrow f_0(980)\rho^0) < -40\%, \quad (62)$$

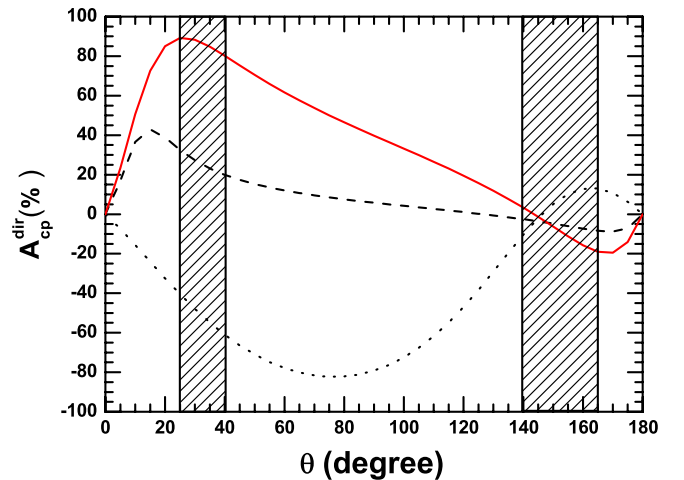


FIG. 4 (color online). The dependence of the direct CP asymmetries for $B^- \rightarrow f_0(980)\rho^-$ (solid curve), $\bar{B}^0 \rightarrow f_0(980)\rho^0$ (dotted curve), and $\bar{B}^0 \rightarrow f_0(980)\omega$ (dashed curve) on the mixing angle θ . The vertical bands show two possible ranges of θ : $25^\circ < \theta < 40^\circ$ and $140^\circ < \theta < 165^\circ$.

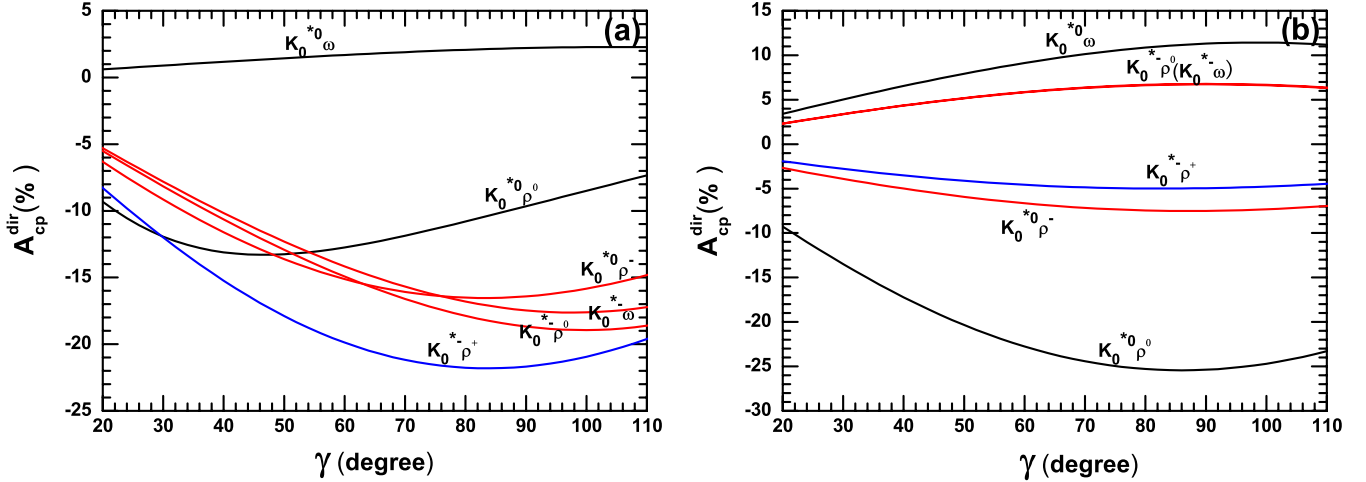


FIG. 5 (color online). The dependence of the direct CP -violating asymmetries for $B^- \rightarrow K_0^{*0} \rho^-, K_0^{*-0} \rho^0, K_0^{*-0} \omega$ and $\bar{B}^0 \rightarrow K_0^{*-0} \rho^+, K_0^{*0} \rho^0, K_0^{*0} \omega$ on the Cabibbo-Kobayashi-Maskawa angle γ .

$$20\% < \mathcal{A}_{CP}^{\text{dir}}(\bar{B}^0 \rightarrow f_0(980)\omega) < 35\%. \quad (63)$$

If the mixing angle is in the range $140^\circ < \theta < 165^\circ$, the direct CP -violating asymmetries of these decays are about

$$-20\% < \mathcal{A}_{CP}^{\text{dir}}(B^- \rightarrow f_0(980)\rho^-) < 5\%, \quad (64)$$

$$-12\% < \mathcal{A}_{CP}^{\text{dir}}(\bar{B}^0 \rightarrow f_0(980)\rho^0) < 15\%, \quad (65)$$

$$-10\% < \mathcal{A}_{CP}^{\text{dir}}(\bar{B}^0 \rightarrow f_0(980)\omega) < 4\%. \quad (66)$$

Certainly, we consider that the gluon component is small and negligible in the meson $f_0(980)$. Our argument is that the neglected gluon component has a small influence on the

TABLE III. Direct CP -violating asymmetries (in units of %) of $B \rightarrow f_0(980)\rho(\omega, \phi)$ and $B \rightarrow K^*(1430)\rho(\omega)$. The errors for these entries correspond to the uncertainties from the scalar meson decay constants, the Gegenbauer moments B_1 and B_3 for the scalar meson, and the B meson shape parameter. Here we still give the predicted direct CP asymmetries of $B \rightarrow f_0(980)\rho(\omega, \phi)$ for the $f_0 - \sigma$ mixing angle $\theta = 20^\circ$.

Mode	Scenario I	Scenario II
$B^- \rightarrow f_0(980)\rho^-$	$85.1^{+0.0+1.8+4.7}_{-0.0-1.8-4.9}$	
$\bar{B}^0 \rightarrow f_0(980)\rho^0$	$-32.4^{+0.0+8.2+3.3}_{-0.0-8.8-8.5}$	
$\bar{B}^0 \rightarrow f_0(980)\phi$	0	
$\bar{B}^0 \rightarrow f_0(980)\omega$	$38.7^{+6.5+6.4+12.0}_{-0.0-7.7-10.3}$	
$B^- \rightarrow \bar{K}_0^{*0}(1430)\rho^-$	$-15.9^{+0.0+1.0+0.8}_{-0.0-1.3-0.8}$	$-7.1^{+0.0+1.6+0.2}_{-0.0-1.0-0.2}$
$B^- \rightarrow K_0^{*-}(1430)\rho^0$	$-16.3^{+0.0+1.8+2.7}_{-0.0-2.0-2.2}$	$6.3^{+0.0+3.9+2.9}_{-0.1-3.8-2.6}$
$B^- \rightarrow K_0^{*-}(1430)\omega$	$-15.4^{+0.2+1.5+2.6}_{-0.3-1.6-2.4}$	$6.2^{+0.0+4.2+3.0}_{-0.0-3.4-2.6}$
$\bar{B}^0 \rightarrow \bar{K}_0^{*0}(1430)\rho^0$	$-12.1^{+0.0+8.5+2.0}_{-0.0-7.8-5.6}$	$-24.2^{+0.2+4.6+3.8}_{-0.0-2.7-4.0}$
$\bar{B}^0 \rightarrow K_0^{*-}(1430)\rho^+$	$-21.0^{+0.0+2.5+1.1}_{-0.0-2.6-0.7}$	$-4.8^{+0.3+0.9+0.4}_{-0.0-0.9-0.5}$
$\bar{B}^0 \rightarrow K_0^{*0}(1430)\omega$	$1.9^{+0.0+0.7+0.6}_{-0.0-0.7-0.0}$	$10.0^{+0.1+2.7+0.9}_{-0.0-2.5-0.9}$

branching ratio, while it has a bit more influence on the CP -violating asymmetry. So if the contribution from the gluon content is included, it will give these direct CP -violating asymmetry values some corrections. As to the decay $\bar{B}^0 \rightarrow f_0(980)\phi$, there is no tree contribution at the leading order, so the direct CP -violating asymmetry is naturally zero.

For the decay $\bar{B}^0 \rightarrow K_0^{*0} \omega$, its direct CP -violating asymmetries for two scenarios are both positive and small (shown in Fig. 5). For the charged decays $B^- \rightarrow \bar{K}_0^{*0}(1430)\rho^-, K_0^{*-}(1430)\rho^0, K_0^{*-}(1430)\omega$, their direct CP asymmetries have similar size in two scenarios (shown in Table III). While in scenario II, the direct CP asymmetry of the decay $B^- \rightarrow \bar{K}_0^{*0}(1430)\rho^-$, whose branching ratio is the largest, has an opposite sign with those of the other two charged decays. It is because there exist contributions from the vector meson emission diagrams in the decays $B^- \rightarrow K_0^{*-}(1430)\rho^0, K_0^{*-}(1430)\omega$, which will flip the signs of their direct CP -violating asymmetry values when the wave function of $K_0^*(1430)$ in scenario II is used, while there are not these kinds of extra contributions in the decay $B^- \rightarrow \bar{K}_0^{*0}(1430)\rho^-$.

V. CONCLUSION

In this paper, we calculate the branching ratios and the CP -violating asymmetries of decays $B \rightarrow f_0(980)\rho(\omega, \phi), K_0^*(1430)\rho(\omega)$ in the PQCD factorization approach. Using the decay constants and light-cone distribution amplitudes derived from QCD sum-rule method, we find that:

- (i) If $f_0(980)$ is purely composed of $n\bar{n}(s\bar{s})$, then the value of $\mathcal{B}(B \rightarrow f_0(n\bar{n})\phi)$ is smaller than that of $\mathcal{B}(\bar{B} \rightarrow f_0(s\bar{s})\phi)$ by about one order for the channel $\bar{B} \rightarrow f_0(s\bar{s})\phi$ [it is contrary to the cases of $\bar{B}^0 \rightarrow f_0(980)\rho(\omega)$]; at the same time, these two branching ratios for $n\bar{n}$ and $s\bar{s}$ components are both very small.

- (ii) In the $b \rightarrow d$ transition processes $B \rightarrow f_0(980)\rho(\omega, \phi)$, the branching ratio of $B^- \rightarrow f_0(980)\rho^-$ is the largest one and its value is possible in the range $(1.0 \sim 2.5) \times 10^{-6}$; the branch ratio of $\bar{B}^0 \rightarrow f_0(980)\rho^0$ is at the order of 10^{-7} . Our predictions for the decays $B^- \rightarrow f_0(980)\rho^-$ and $\bar{B}^0 \rightarrow f_0(980)\omega$ are smaller than the experimental upper limits, but not far away from them.
- (iii) In the $b \rightarrow s$ transition processes $B \rightarrow K_0^*\rho(\omega)$, there exists a small difference for the values of their branch ratios, and most of them are in the range of $(3 \sim 5) \times 10^{-6}$ for scenario I, $(7 \sim 10) \times 10^{-6}$ for scenario II.
- (iv) In scenario I, the branch ratio of $\bar{B}^0 \rightarrow K_0^{*0}(1430)\rho^0$ is the smallest one in these $b \rightarrow s$ transition processes, and its value is at the order of 10^{-7} in scenario I. Certainly, we only calculate the leading order diagrams, and do not consider the higher order corrections. If the future experimental value about this channel is larger than our prediction, say 10^{-6} , it indicates that this decay might be more sensitive to next-to-leading order corrections, which is similar to the decays $B^0 \rightarrow \pi^0\pi^0, \rho^0\rho^0$. On the other side, the decay $\bar{B}^0 \rightarrow K_0^{*0}(1430)\omega$ arrives at a large rate in our leading order calculations. We expect that its value will be smaller after considering next-to-leading order corrections.
- (v) The direct CP -violating asymmetries of decays $B \rightarrow f_0(980)\rho(\omega)$ have a strong dependent on the mixing angle θ : they are large in the range of $25^\circ < \theta < 40^\circ$ and small in the range of $140^\circ < \theta < 165^\circ$, while the direct CP -violating asymmetry amplitudes of decays $B \rightarrow K_0^*(1430)\rho(\omega)$ are not large in both scenarios and most of them are less than 20%.

ACKNOWLEDGMENTS

This work is partly supported by Foundation of Henan University of Technology under Grant No. 150374.

-
- [1] N. A. Tornqvist, *Phys. Rev. Lett.* **49**, 624 (1982).
- [2] G. L. Jaffe, *Phys. Rev. D* **15**, 267 (1977); **15**, 281 (1977); A. L. Kataev, *Phys. At. Nucl.* **68**, 567 (2005); *Yad. Fiz.* **68**, 597 (2005); A. Vijande, A. Valcarce, F. Fernandez, and B. Silvestre-Brac, *Phys. Rev. D* **72**, 034025(E) (2005).
- [3] J. Weinstein and N. Isgur, *Phys. Rev. Lett.* **48**, 659 (1982); *Phys. Rev. D* **27**, 588 (1983); **41**, 2236 (1990); M. P. Locher *et al.*, *Eur. Phys. J. C* **4**, 317 (1998).
- [4] V. Baru *et al.*, *Phys. Lett. B* **586**, 53 (2004).
- [5] L. Celenza *et al.*, *Phys. Rev. C* **61**, 035201 (2000).
- [6] M. Strohmeier-Presicek *et al.*, *Phys. Rev. D* **60**, 054010 (1999).
- [7] F. E. Close and A. Kirk, *Phys. Lett. B* **483**, 345 (2000).
- [8] H. Y. Cheng, C. K. Chua, and K. C. Yang, *Phys. Rev. D* **73**, 014017 (2006).
- [9] H. Y. Cheng, C. K. Chua, and K. C. Yang, *Phys. Rev. D* **77**, 014034 (2008).
- [10] W. Wang, Y. L. Shen, Y. Li, and C. D. Lü, *Phys. Rev. D* **74**, 114010 (2006).
- [11] O. Abreu *et al.* (DELPHI Collaboration), *Phys. Lett. B* **449**, 364 (1999); A. Aloisio *et al.* (KLOE Collaboration), *Phys. Lett. B* **537**, 21 (2002); M. N. Achasov *et al.*, *Phys. Lett. B* **485**, 349 (2000).
- [12] A. V. Anisovich, V. V. Anisovich, and V. A. Nikonov, *Eur. Phys. J. A* **12**, 103 (2001); *Phys. At. Nucl.* **65**, 497 (2002).
- [13] R. Kaminski, L. Lesniak, and B. Loiseau, *Eur. Phys. J. C* **9**, 141 (1999).
- [14] A. Garmash *et al.* (Belle Collaboration), *Phys. Rev. D* **71**, 092003 (2005).
- [15] A. Garmash *et al.* (Belle Collaboration), *Phys. Rev. Lett.* **96**, 251803 (2006); **94**, 041802 (2005).
- [16] B. Aubert, *et al.* (BABAR Collaboration), *Phys. Rev. D* **73**, 031101 (2006).
- [17] B. Aubert *et al.* (BABAR Collaboration), *Phys. Rev. D* **72**, 072003 (2005); **71**, 052001 (2005).
- [18] C. Amsler *et al.* (Particle Data Group), *Phys. Lett. B* **667**, 1 (2008);
- [19] B. Aubert, *et al.* (BABAR Collaboration), *Phys. Rev. Lett.* **101**, 201801 (2008).
- [20] C. D. Lu and M. Z. Yang, *Eur. Phys. J. C* **28**, 515 (2003).
- [21] W. M. Yao *et al.* (Particle Data Group), *J. Phys. G* **33**, 1 (2006).
- [22] P. Ball, G. W. Jones, and R. Zwicky, *Phys. Rev. D* **75**, 054004 (2007).
- [23] P. Ball and R. Zwicky, *Phys. Rev. D* **71**, 014029 (2005); *J. High Energy Phys.* 04 (2006) 046; P. Ball and G. W. Jones, *J. High Energy Phys.* 03 (2007) 069.
- [24] H. N. Li, *Phys. Rev. D* **66**, 094010 (2002).
- [25] H. N. Li and B. Tseng, *Phys. Rev. D* **57**, 443 (1998).
- [26] G. Buchalla, A. J. Buras, and M. E. Lautenbacher, *Rev. Mod. Phys.* **68**, 1125 (1996).
- [27] Z. Q. Zhang and J. D. Zhang, *Eur. Phys. J. C* **67**, 163 (2010).
- [28] Z. J. Xiao, Z. Q. Zhang, X. Liu, and L. B. Guo, *Phys. Rev. D* **78**, 114001 (2008).
- [29] P. del Amo Sanchez *et al.* (BABAR Collaboration), arXiv: hep-ex/1005.1096.
- [30] C. S. Kim, Y. Li, and W. Wang, *Phys. Rev. D* **81**, 074014 (2010).